Chapter 3

Nanocrystallization of the $Cd_3Al_2Ge_3O_{12}$ Garnet in Glasses of the CdO-TeO_2-GeO_2 System

Josefina Alvarado Rivera,
Carlos Guadalupe Pérez Hernández,
María Elena Zayas and Enrique Álvarez

Additional information is available at the end of the chapter

http://dx.doi.org/10.5772/intechopen.73295

Abstract

In this study, a series of glasses of the system xCdO-10TeO_2-(90−x)GeO_2 were fabricated, varying the modifier oxide content from 10 to 80 wt%. According to XRD analysis, partial crystallization occurred for the glass 60CdO.10TeO_2.30GeO_2 presenting the formation of GeO_2 and $CdTeO_3$; the 70CdO.10TeO_2.20GeO_2 glass shows sharp diffraction peaks corresponding to the $Cd_3Al_2Ge_3O_{12}$ garnet crystalline phase. Transmission electron microscopy showed that the garnet crystals have sizes below 20 nm. At the highest concentration of CdO (80 wt%), a transparent orange glass can be obtained, and this sample can be identified as an inverted glass where CdO participates as a network former. The optical band gap of the glasses decreases as CdO content increases from 3.91 to 3.0 eV. In general, all glasses show a typical broad emission when excited with UV light (325 nm); chromatic coordinates were calculated and pointed out the presence of emissions in the white, green, and yellow regions. In summary, the obtained glasses are a promising material for IR technologies, nonlinear optics, and design of solid state lighting devices.

Keywords: tellurite, germanates, nanocrystals, photoluminescence, inverted glasses

1. Introduction

As technology keeps evolving, particularly in the optics and telecommunication applications, materials with very special properties and capabilities like specific spectral operation ranges, high refractive index, and low phonon energy are needed [1]. Herein, silicon oxide (SiO_2), germanium oxide (GeO_2), tellurium oxide (TeO_2), vanadium pentoxide (V_2O_5), cadmium sulfide (CdS), to name a few, have been used to fabricate special glasses with optical

properties adequate to their final application. The main characteristic of the mentioned compounds is that they are glass network formers, and alkali oxides (Na_2O, CaO, K_2O, and MgO) and metallic oxides (like ZnO and Fe_2O_3) are network modifiers. Tellurium oxide is a special case of a glass former; it has been proved that the structural unit that constitutes the network is of octahedral coordination nature, which deviates from the classical structural model of tetrahedral coordination. Zachariasen postulated through empirical observation that cations surrounded by four oxygens in a tetrahedral geometry could form glass [2]. However, it has been found by several authors that some glasses (including TeO_2-based glasses) do not follow this rule. Goldschmidt [3] pointed out the important role of the radius ratio for glass-forming oxides, which is the ratio between the ionic radius of the cation and oxygen atoms, r_C/r_O, and it has values of 0.2–0.4 for tetrahedral coordination. Afterwards, Zachariasen took these concepts as a base to develop a model for glass formation, where tetrahedral units share oxygen atoms at the corners constructing a continuous glass network. The SiO_2 glass is formed by a tridimensional network of $(SiO_4)^{4-}$ connected through oxygen atoms at the corners, where at least three corners participate in the irregular network, which does not have translational periodicity. That network is "interrupted" where other cations from modifier compounds (X) are added to glass, forming Si—O—X bonds terminating the connectivity. Some cations can participate forming either as the glass network or as modifiers like Al, Be, Zr, Zn, Cd, and Pb, and this change in behavior will depend on their concentration and their interaction with other components in the glass [4].

For decades, continuous research of new glass systems has led to modify the rules of the classic glass model. Lead orthosilicate glass ($PbSiO_4$) is a glass that does not follow Zachariasen's rules since Pb^{2+} has an octahedral coordination and a large ionic radius (r = 132 pm). In addition, it is possible to fabricate borate glasses with low concentration of B_2O_3, which forms rutile-like octahedral units [5]. The term "inverted glasses" first appeared in the work of Stevels [6] regarding a metasilicate glass formed by three isolated coupled SiO_4 units instead of a continuous network. Thus, a glass that does not follow the classical model and whose network is formed by polyhedra of modifier cations in their majority is called an inverted glass. Some examples are tellurites in which Te ions with a six-fold coordination number form distorted octahedra interconnected between oxygens at the corners [2]. As it is the case of $CaO–Na_2O–MgO–P_2O_5$ glasses with a concentration of MgO higher than 60% mol, Mg—O coordination number changes from ~6 to ~5, which is lower than that of its crystalline form, allowing MgO to change its role to that of a glass former [7].

Finally, applications of inverted glasses will depend on the chemical composition of each vitreous system, and there is a variety of them. For example, for vitreous systems with network modifiers like CdO, ZnO, PbO, and MgO, among others, in high proportions, they are characterized by their good optical properties, and these glasses are attractive for optical devices and laser designs [7]. Furthermore, the introduction of rare earth oxides to germanate tellurite glasses together with their transparency in the infrared region makes them interesting for multiband amplifiers [8].

In this work, the effect of high contents of CdO on the crystallization and formation of inverted glasses of the CdO-TeO_2-GeO_2 system was studied. It was expected that as the

http://dx.doi.org/10.5772/intechopen.73295

modifier oxide increases, devitrification of the glasses will very likely occur. However, as Cd^{2+} cations can coordinate in octahedral units, it is possible that its role as modifier can change to that of an intermediate. Furthermore, the energy band gap of the glasses was calculated from optical absorption spectra. For possible applications in solid state lighting, photoluminescence under UV light excitation of amorphous and crystallized samples was studied.

2. Experimental procedure

2.1. Glass fabrication

A series of eight glasses with a concentration of xCdO-10TeO_2-(100−x)GeO_2, with x values from 80 to 10 wt%, was fabricated. This series of glasses is localized in the rich GeO_2 region of the ternary system diagram as is depicted in **Figure 1**. All oxide powders were purchased by Sigma Aldrich with a >98% purity and were used without further purification (see **Table 1**). The appropriate amount of powders was mixed and homogenized with acetone and then left overnight to dry at room temperature. Afterwards, the batches were melted at 1350°C for 20 min in alumina crucibles, and then the melts were quenched in bronze molds. The density of the glasses was determined using Archimedes' principle estimating the difference between the body weight and the apparent immersed weight. All these measurements were carried out at room temperatures, and distilled water was used as reference immersion liquid.

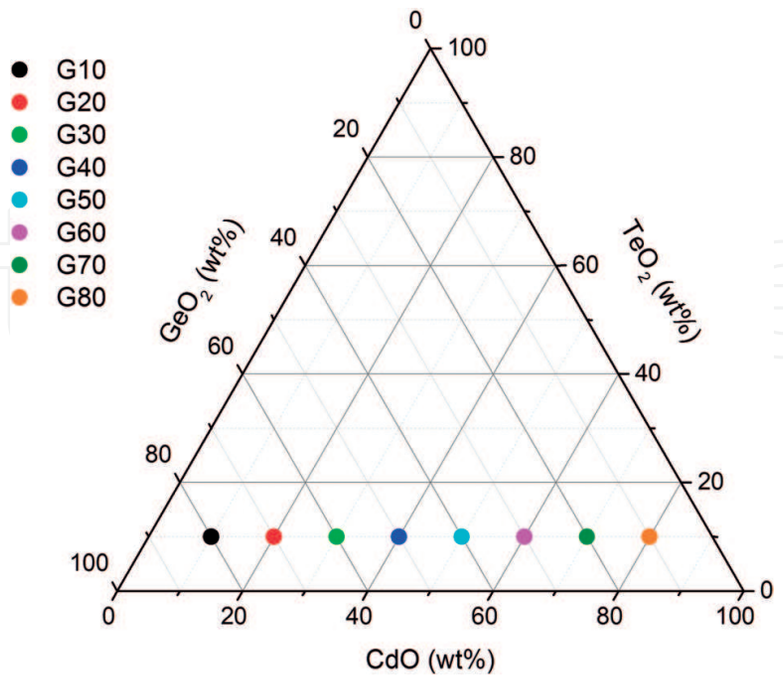

Figure 1. Nominal composition of the studied glass series displayed on the CdO-TeO_2-GeO_2 ternary diagram.

Label	CdO (wt%)	TeO_2 (wt%)	GeO_2 (wt%)	Obtained glasses
G10	10	10	80	
G20	20	10	70	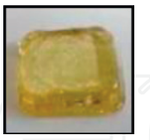
G30	30	10	60	
G40	40	10	50	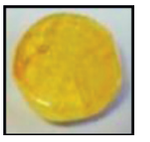
G50	50	10	40	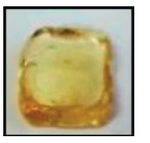
G60	60	10	30	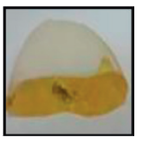
G70	70	10	20	
G80	80	10	10	

Table 1. Nominal compositions of the glass series.

2.2. Material characterization

The fabricated glasses were characterized by several techniques to study their structural, thermal, and photoluminescent properties. Differential thermal analysis (DTA) was performed in a TA Instrument SDT2960; the samples were heated in an alumina crucible at a rate of 10°C/min from ambient temperature to 1200°C. X-ray diffraction (XRD) was carried out by a Bruker D8 ADVANCE diffractometer. Raman spectroscopy was performed using a 632 nm laser in a Horiba Jobin-Yvon LABRAM HR800 spectrometer. Fourier transform infrared (FTIR) was measured in a Perkin-Elmer model spectrum two spectrometer in the range of 4000 to 500 cm^{-1}. X-ray photoelectron spectroscopy (XPS) of selected samples was also performed

in a Perkin Elmer PHI 5100 spectrometer with a dual Al/Mg anode, Al kα X-ray of 1436 eV excitation radiation was used for the samples characterization, and charge displacement of the samples was corrected using C 1 s peak position at 284.8 eV. Sample G70, which showed a great devitrification, was characterized by transmission electron microscopy to observe the size of the crystalline phase formed in the glass matrix. Photoluminescence of the glasses was monitored in a Horiba Jobin-Yvon FluoroLog-3 spectrofluorometer using different excitation wavelengths in the UV region.

3. Results and discussion

The obtained glasses were of yellowish transparent color (**Table 1**) and for concentrations of CdO of 60 and 70 wt% presented devitrification, at 80 wt% CdO, an orange transparent glass was obtained, and it can be considered an inverted glass. Formation of glass at greater proportions of the modifier oxide was not expected according to Zachariasen's rules. Instead, the formation of a crystalline phase rich in Cd was the most plausible outcome. However, it was possible to obtain a partially devitrified glass, a transparent glass, and a crystalline sample. It can be seen that at 60 wt% CdO, devitrification at the top of the sample is visible, and a white crystalline phase was formed.

3.1. Density and thermal properties

Density, glass transition (T_g), crystallization (T_c), and melting (T_m) temperature values for each glass are shown in **Table 2**. In general, density increases with CdO content, except for samples C20 and C30 where an anomaly is observed (**Figure 2a**). At 30 wt% CdO, the glass density reaches a minimum value and then increases steadily up to 80 wt%. This behavior is consistent with the "germanate anomaly" in alkali germanate glasses where at a certain concentration of alkali oxides, the increment in nonbonding oxides (NBO) affects the glass density [9, 10]. At higher concentrations of CdO, an increase in density occurs probably because of the large Cd ion; such behavior has been previously reported in glasses, crystals, and solutions

Glass	E_g (eV)	CdO (wt%)
C10	3.90	10
C20	3.93	20
C30	3.88	30
C40	3.84	40
C50	3.77	50
C60	3.74	60
C70	3.61	70
C80	3.01	80

Table 2. Optical energy band gap, E_g, of the glasses.

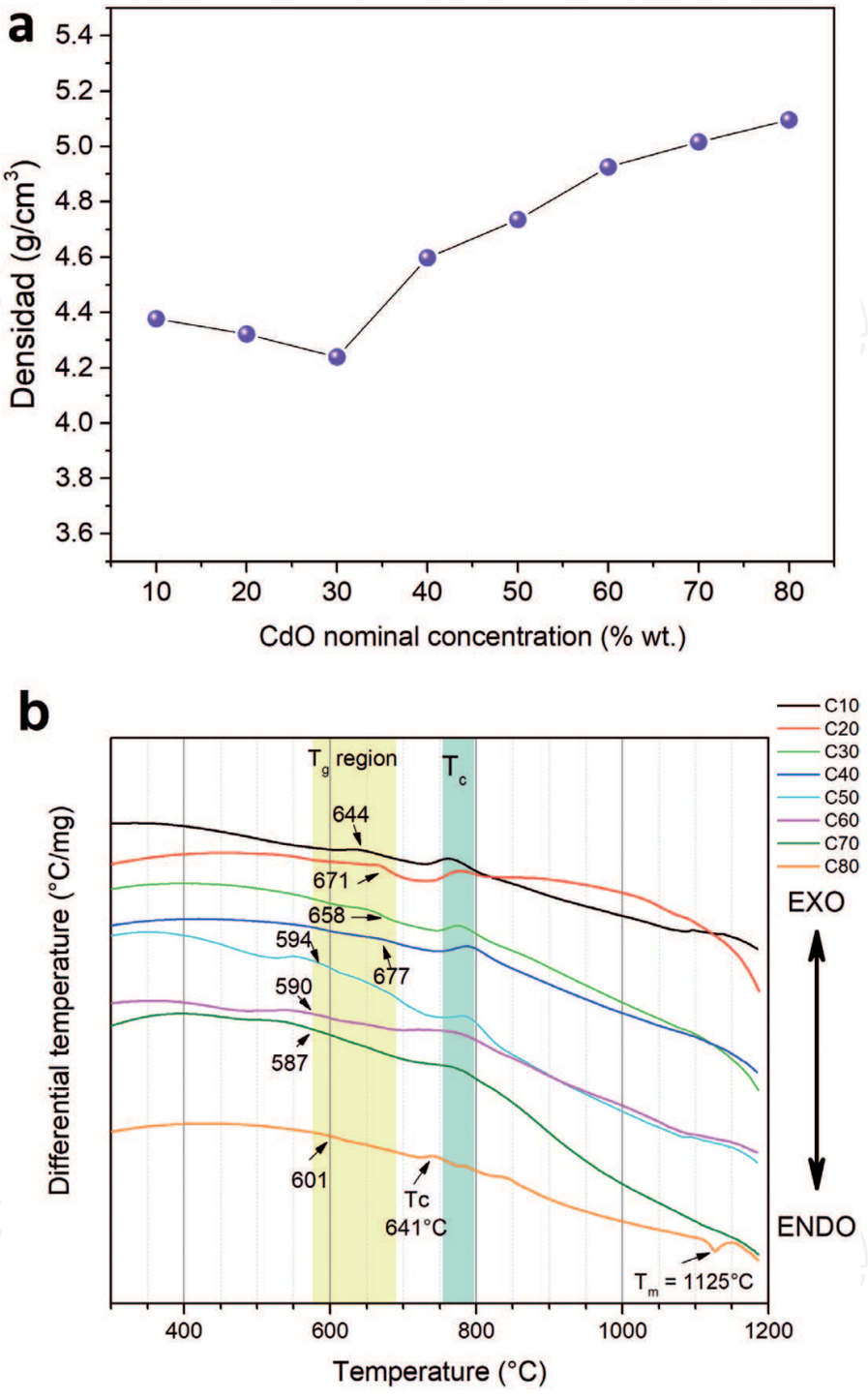

Figure 2. (a) The density of the glasses as a function of CdO concentration and (b) DTA curves of the analyzed glasses.

[11, 12]. DTA curves of the fabricated glasses are presented in **Figure 2b**; the exothermal peaks are associated to T_g or T_c, and there is one endothermic peak for glass C80, which corresponds to a melting point. The samples below 50 wt% GeO_2 have the highest values of T_g and T_c and decrease for the glasses with a higher concentration of CdO; sample C80 is the only one, in the range of analysis, that presents a melting temperature at 1125°C.

http://dx.doi.org/10.5772/intechopen.73295

3.2. Structural characterization

3.2.1. XRD

Diffraction patterns of all samples are shown in **Figure 3**, and they are separated into three parts. Samples that showed a broad band without diffraction peaks indicating their amorphous nature are exhibited in **Figure 3a**, which were the glasses richest in GeO_2 up to 50 wt%, and C80 sample presented with the highest concentration of CdO. Thus, we obtained an inverted glass where CdO changes its role from modifier to glass network former together with GeO_2 and TeO_2; only a few systems have shown this behavior [7, 13]. Sample G30 (**Figure 3b**) presented a diffraction peak at 2θ = 23.3° related to the orthorhombic phase $Al_6Ge_2O_{13}$. On the other hand, C60 (**Figure 3b**) presented several defined diffraction peaks overlapped with the glassy matrix broad band, and it corresponds with a cadmium aluminum germanate ($Cd_3Al_2Ge_3O_{12}$), which has a garnet crystalline structure. Aluminum incorporation into the glass has its origin from the high-alumina crucible corrosion during the melting process at 1350°C. Furthermore,

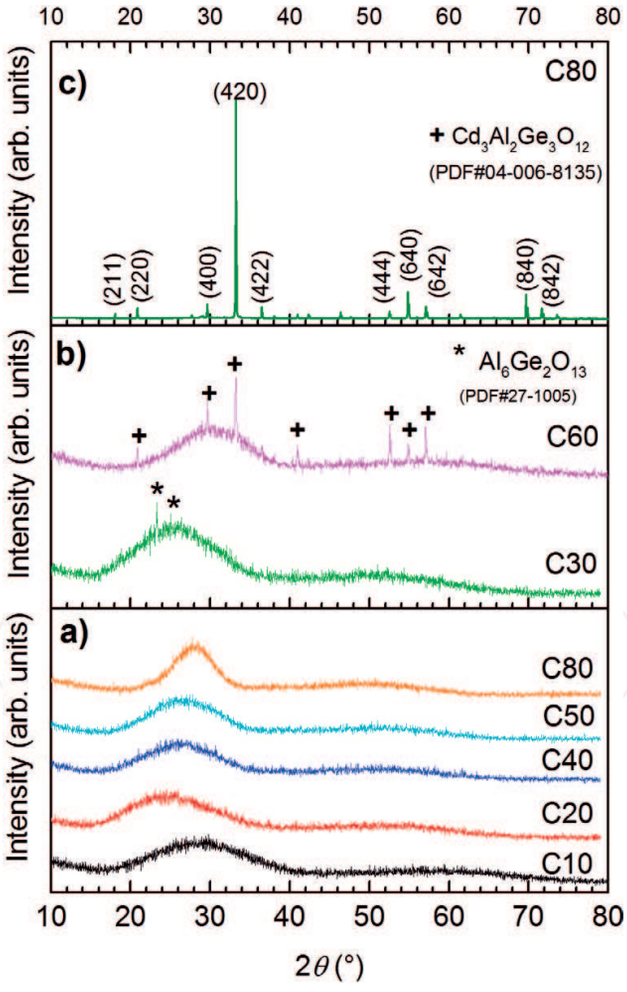

Figure 3. Diffraction patterns of (a) samples that show the characteristic broad diffraction band of amorphous materials, (b) C30 and C60 glasses with phase crystallization, and (c) sample C70 evidencing a complete devitrification and formation of $Cd_3Al_2Ge_3O_{12}$.

sample C70 evidenced well-defined sharp diffraction peaks assigned to the $Cd_3Al_2Ge_3O_{12}$ garnet. It is interesting that both crystalline phases found in the glasses have aluminum in their chemical composition, and phases with only the glasses original constituents (like $CdTeO_3$ or $CdGeO_3$) were not detected.

3.3. Raman spectra

Evolution of the glass structure was explored using Raman spectroscopy, and the spectra are presented in **Figure 4**. Samples C60 and C70 were fabricated a second time to confirm if it was possible to obtain glasses with those compositions, and two yellowish transparent glasses were obtained. The bands related to Ge—O—Ge bonds, GeO_4 and GeO_6 structural units, and Te—O—Te bonds appear in the 400–600 cm^{-1} region [10, 14]. As the concentration of GeO_2 reduces, this broad band changes its intensity until it vanishes for samples C70 and C80. The band within the range of 600 to 900 cm^{-1} exhibits changes in intensity as GeO_2 decreases in content. In the same region, bands for both Ge—O—Ge and Te—O—Te bonds can be found. The maximum shift toward lower wavenumber values from 740 to 760 cm^{-1} is associated with $Te—O^-$ bonds in TeO_{3+1}/TeO_3 groups for the C70 and C80 samples [14–16]. As for glasses C10 to C60, a shift toward 792 cm^{-1} occurs, and in this region, absorption bands related to NBOS from GeO_4 groups are found. Thus, GeO_4 groups can be distinguished in two types, Q^3 (1 NBO) and Q^2 (2 NBOs) units, and the absorption bands related to them appear at ~790 and ~870 cm^{-1}, respectively [10]. Henderson [9] studied the evolution of Q^3 and Q^2 units as a function of the increment in the concentration of alkali oxides; results show that the absorption

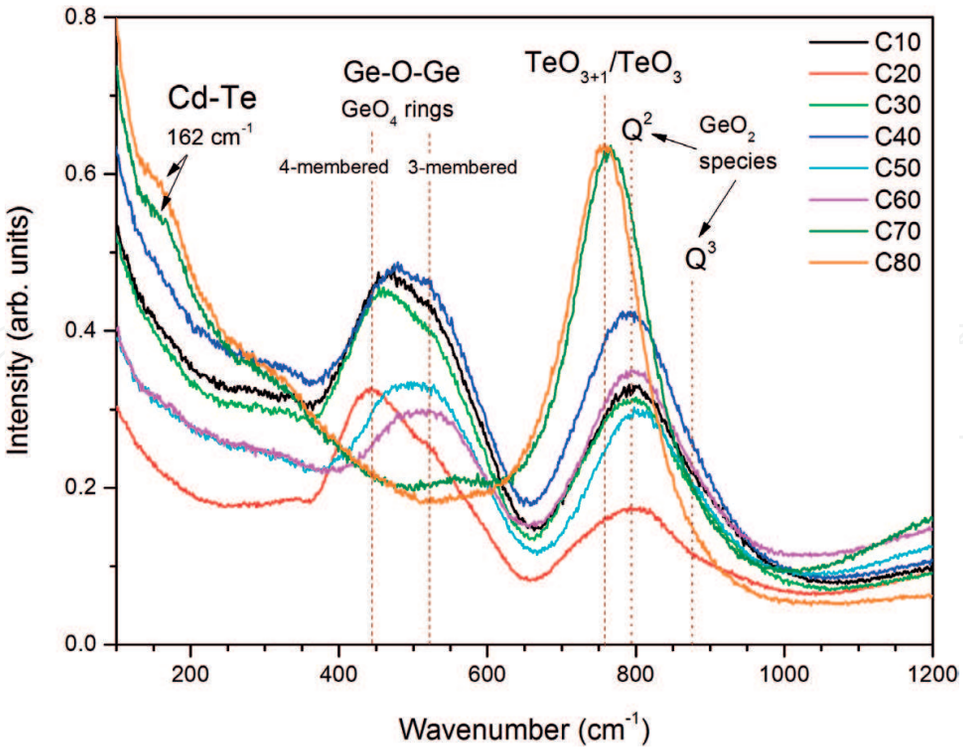

Figure 4. Raman spectra of the glasses; two main broad bands dominate the spectra features and are related to GeO_4 and TeO_{3+1}/TeO_3 structural units present in the glass network.

band of Q^3 units is more intense at higher contents of the modifiers, and a less intense band of Q^2 units is also detected. Thus, Cd^{2+} ions are introducing a larger amount of NBO oxides, as a consequence of its high coordination number, and then at concentrations of 70 and 80 wt%, the network is "inverted" as CdO becomes the glass former.

A third small band at lower wavenumber values (162 cm^{-1}) only appears for samples C70 and C80, and it is related to Cd—Te bonds [17, 18]. However, no crystalline formation of CdTe was identified by XRD. Then, we can only infer that in those rich CdO samples part of Cd^{2+} ions are still participating as modifiers and are also coordinated with Te in TeO_{3+1}/TeO_3 groups due to the lone pair of electrons of Te atoms.

3.4. Infrared spectra

FTIR spectra of the glasses under study (**Figure 5**) show a very broad band in the range of 600–900 cm^{-1} in which Ge—O—Ge and Te—O—Te bond vibrations are found. As it was observed from Raman spectra, CdO induces a change in coordination of germanium ions from four to six, and absorption bands of GeO_4 and GeO_6 units appear around ~880 and ~715 cm^{-1}, respectively [1, 10, 19, 20]. CdO induces a change in coordination number of Ge from four to six, GeO_4 groups disappear at higher concentrations of the modifier (C70, C80), and only a small and smooth band of GeO_6 remains [1, 21]. Te—O—Te bonds in TeO_4 network absorption band appears around 780 cm^{-1}, and NBOs in Te—O^- or Te═O from TeO_{3+1}/TeO_3 units are located at 820 cm^{-1} [21]. For glasses C70 and C80, a very small band at 763 cm^{-1} is still visible, and it

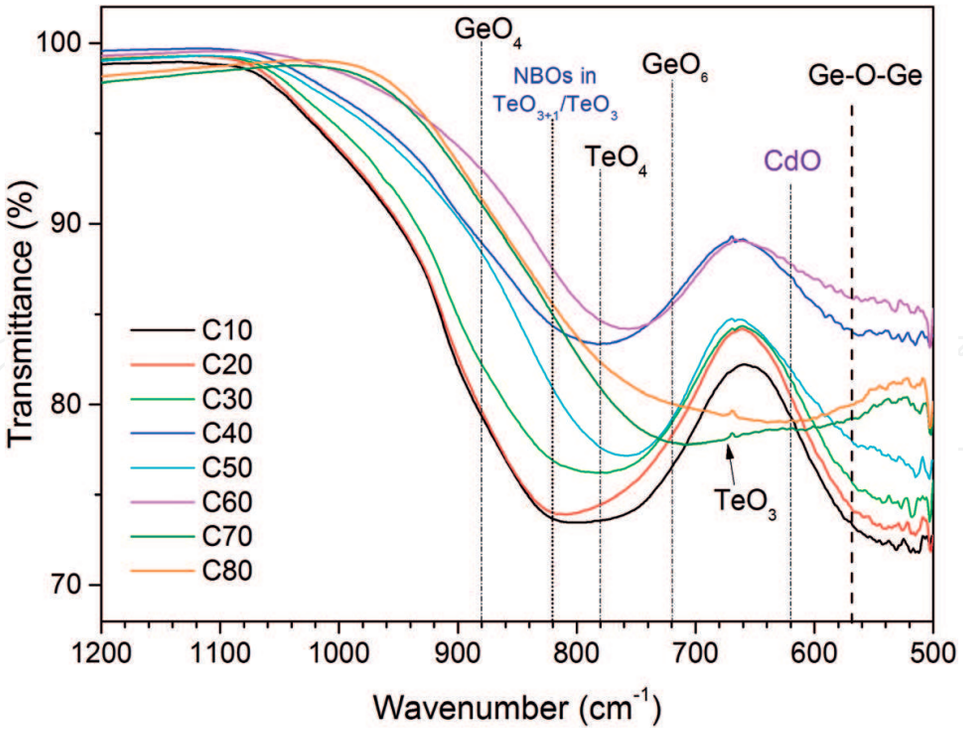

Figure 5. FTIR spectra of all CdO-TeO_2-GeO_2 glasses showing two broad bands at 700–900 and 500–650 cm^{-1}. The former is composed of the bands related to GeO_4, GeO_6, and Te—O—Te bonds in TeO_4 and TeO_{3+1}/TeO_3 groups; the latter corresponds to Ge—O—Ge of Ge ions in six-fold and four-fold coordination.

corresponds to TeO_3 groups, this band does not appear for lower CdO concentrations [1]. It is difficult to determine the band's positions ought to the overlapping of both Te—O—Te and Ge—O—Ge bonds absorption bands. Thus, a position shift probably occurs as the concentration of GeO_2 and CdO changes. At this respect, absorption bands of Cd-O bonds in CdO are reported to appear at 620 cm^{-1} which is visible only for samples C79 and C80 [22]. In the low wavenumber region, around 500–600 cm^{-1}, there is an absorption band of symmetric stretching vibrations of Ge—O—Ge at 566 cm^{-1} [23]. From this analysis, we can confirm that Cd—O bonds constitute the glass structure of the inverted glasses and there are some remaining GeO_6 and TeO_3 groups.

3.5. XPS

At this point, we have established that CdO has a very important role in the structural change of the glass network. High-resolution XPS analysis was performed on C10, the lowest in CdO concentration, and C60, C70, and C80, Cd 3d, Te 3d, Ge 3d, and Al 2p photoelectron lines spectra are presented in **Figure 6**. In the case of Cd 3d spin-orbit doublet (**Figure 6a**), peak positions are presented in 405.3, 405.4, 405.1, 405.15 and 412.1, 412.05, 411.9, 412 eV, respectively, for sample C10, C60, C70, and C80. Those values can be referred to Cd^{2+} ions as it was reported by Moholkar [24], confirming that the above 60 wt% of CdO changes its role to that of a glass former. **Figure 6b** presents Te $3d_{5/2}$ and Te $3d_{3/2}$ doublet in which each photoelectron lines are composed of two well-defined peaks, evidencing that Te ions are chemically bonded in two distinct species. It is noticeable that the peak positions do not shift in binding energy for all analyzed compositions, and they are at 572.5, 575.8 and 583, 586.3 eV for Cd $3d_{5/2}$ and $3d_{3/2}$, respectively. Previous XPS analysis on tellurite glasses showed that Te $3d_{5/2}$ position is in the range of 575.6–576.9 eV and is associated to Te^{4+} [25–27]; the peak intensity varies with CdO concentration. It is the least intense at 60 wt% and then increases for samples richest in CdO. The peaks at 572.5 and 583 eV (Cd $3d_{5/2}$ and $3d_{3/2}$) are related to CdTe [27], and for glasses, C70 and C80, a band related to CdTe was found in Raman analysis. A shift toward lower energy values of the core level peak indicates that Cd^{2+} undergoes an increment in its charge distribution sphere, and this is a very polarizable cation. It is worth to notice that the peaks related to CdTe are more intense for the sample C10 (only 10 wt% of CdO) than those for rich CdO glasses. Thus, Cd^{2+} ions do not participate as a traditional modifier oxide, only interacting with oxygen in Ge—O^- and Te—O^- terminal bonds. It could be possible that cadmium ions are attracted to the lone pair of electrons of Te in $TeO_{3+1,}$ and TeO_3 groups, forming O—Te—Cd complexes in which Cd ions are interrupting the network connectivity. Further analysis is needed to perform to understand how Cd^{2+} ions are interacting and changing the glass network and affecting the optical properties of the glasses in this system.

Ge 3d core-level peak spectra of the analyzed glasses are displayed in **Figure 6c**. A shift toward lower binding energy values (from 32.15 to 30.9 eV) as CdO concentration increases can be distinguished, and it is associated with Ge coordination change from four to six [28]. Al 2p photoelectron line is shown in **Figure 6d** for C60, C70, and C80 glasses only, and no aluminum incorporation was detected for sample C10. Aluminum was not detected in Raman or FTIR

spectroscopies; Al 2p peak position is 73.9 eV for C60 and C70 samples and corresponds to Al—O bonds in Al_2O_3 [29]. For C80 glass, the peak shifts toward 72.6 eV, which is related to Al^0, and this indicates that aluminum is probably not participating in glass network formation.

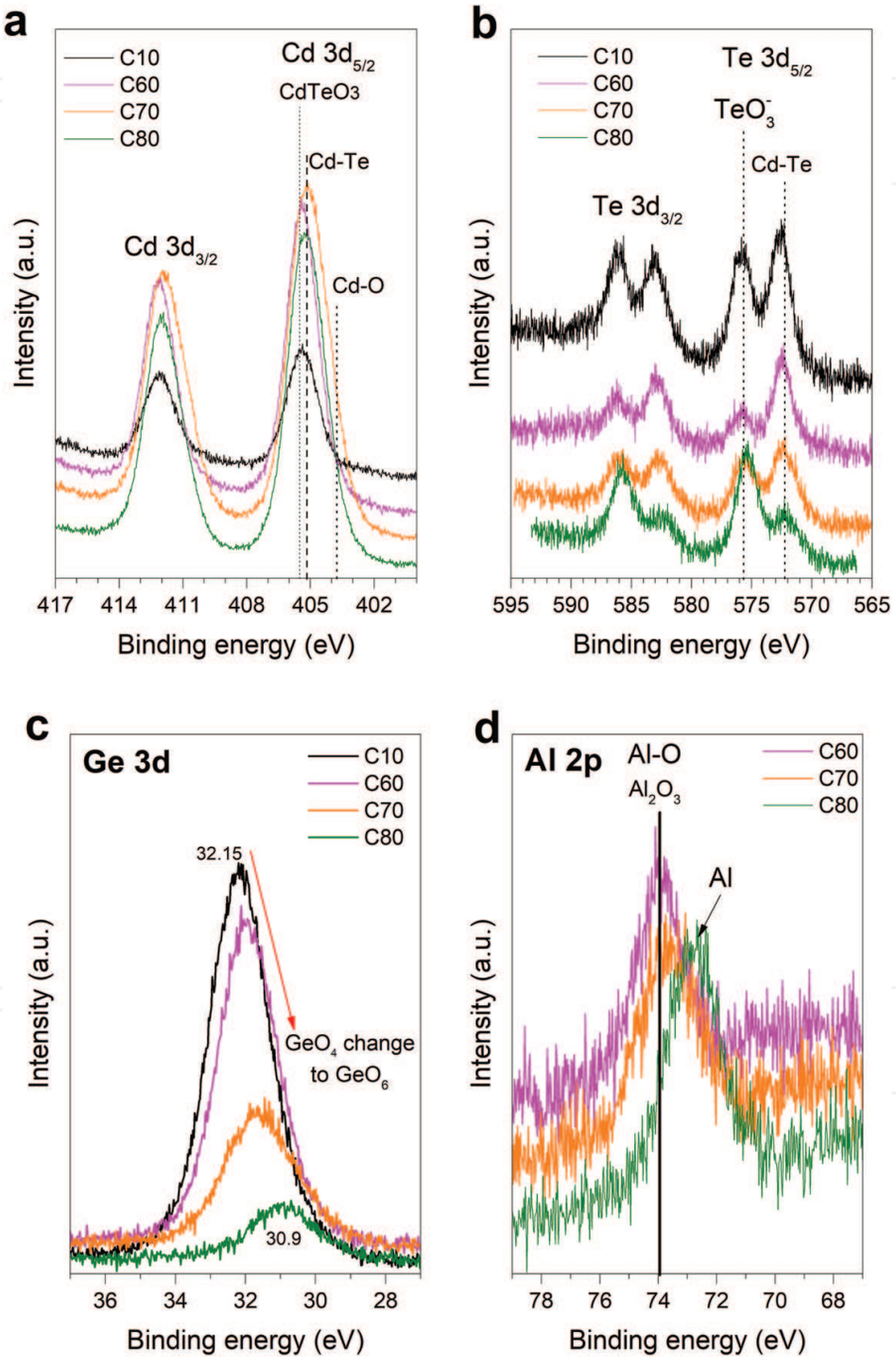

Figure 6. High-resolution XPS spectra of samples C10, C60, C70, and C80 of Ge 3d and Al 2p peaks; and Cd 3d and Te 3d spin-orbit doublets.

3.6. UV-Vis

Optical absorption of the glasses is shown in **Figure 7** and energy band gap by Tauc's method by plotting $(h\nu\alpha)^n$ vs. $(h\nu - E_g)$ was estimated; $h\nu$ is the photon energy, α is the absorption coefficient, and n = 1/2 is the amorphous materials. The determined values for E_g are listed in **Table 3**. As it is seen, CdO has a significant effect on the energy band gap of the glasses that decreases as the content of the modifier oxide increases, from 3.90 to 3.01 eV for 10 and 80 wt% of CdO, respectively. This behavior can be related to CdO semiconductor properties that modify the dielectric constant of the host material; previous investigations show that Cd ions can exhibit such significant decrease in E_g values [30, 31].

3.7. Photoluminescence

Glass photoluminescence (PL) was monitored using a 370 nm UV excitation light; this wavelength was selected according to the emission of commercial chips used as UV pumps in LEDs, which is in the range of 360–375 nm. PL emission spectra of the glasses show a broad band emission covering the visible spectral range (400–700 m) and are presented in **Figure 8**. The effect of CdO concentration on the glass structure and, therefore, in the light emission of the glasses is evident; the spectral features show variations through all concentrations. Luminescence in glasses has its origin in "defects" from a chemical standpoint because a glass structure lacks periodicity and symmetry operations. Emission spectra of CdO-TeO_2-GeO_2 glasses are very complex as a consequence of the several components and related defects that constitute their glass structure.

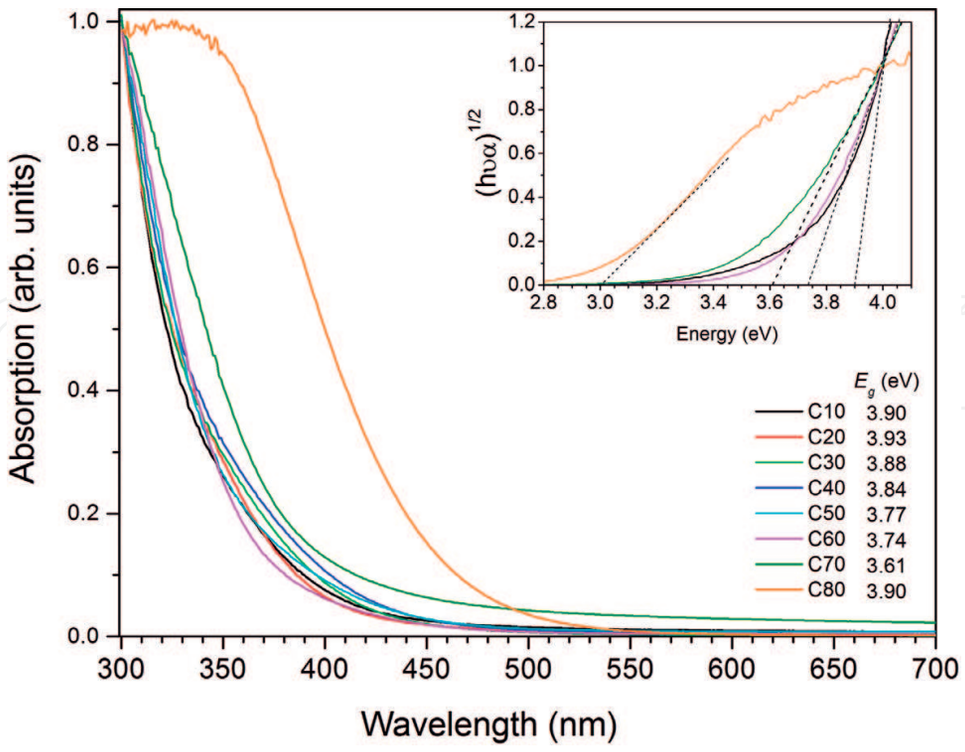

Figure 7. UV–Vis absorption spectra of the glasses; the inset shows $(h\nu\alpha)^n$ vs. $(h\nu - E_g)$ of some samples and their corresponding tangent line to the point of inflection of the curve to the hν at the point of intersection.

http://dx.doi.org/10.5772/intechopen.73295

Glass	E_g (eV)	CdO (% wt.)
C10	3.90	10
C20	3.93	20
C30	3.88	30
C40	3.84	40
C50	3.77	50
C60	3.74	60
C70	3.61	70
C80	3.01	80

Table 3. Estimated energy band gap, E_g, of the CdO-TeO_2-GeO_2 glasses.

In general, all sample spectra show a band maximum that gradually shifts from 555 to 585 nm as CdO content increases. At lower wavelengths, C10 and C40 show a distinct shoulder around 449 nm, and for sample C20, shifts to 455 nm and its intensity decrease. C50 and C60 do not show a shoulder, only a broad band at 571 and 576, respectively, indicating that the glass structure did change and the defect causing that feature disappeared. Sample C70 has a band shoulder at 476 nm, as it was mentioned above, and at this composition, the structure starts to invert from a GeO_2 to a CdO network. Sample C30 shows a small emission band at 415 nm, and C80 presents a structured band with two maxima at 422 and 434 nm, and it is more intense than the main broad band in other glasses.

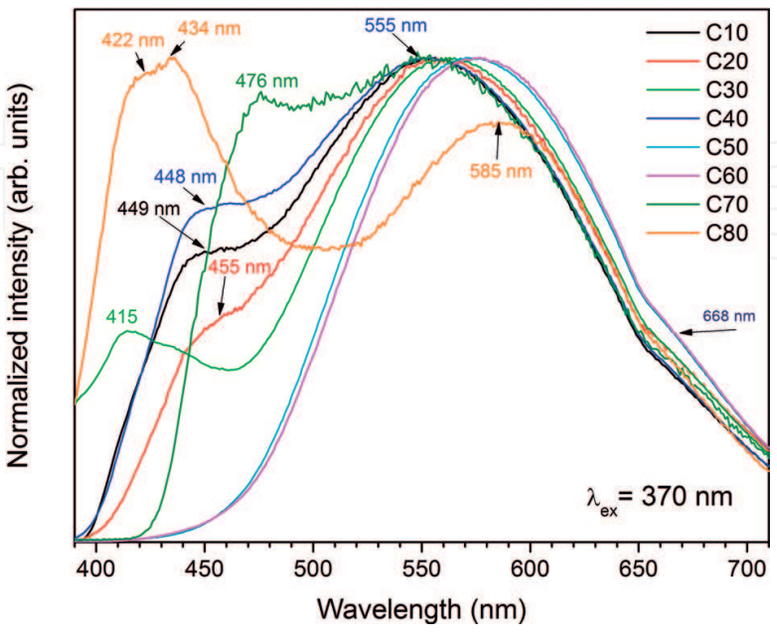

Figure 8. PL emission spectra of the glasses monitored using an excitation wavelength of 370 nm.

It has been thoroughly studied that in GeO_2 glasses, the Ge^{2+} emission center (defect) presents two emission bands at 300 and 395 nm under UV light (254 and 330 nm), which is from the $S_1 \rightarrow T_0$ and $T_1 \rightarrow T_0$ transitions [32]. However, those bands related to GeO_2 glass do not appear in the range of analysis, and it seems that, for samples C30 and C80, emission spectra extend beyond the monitored range toward UV region. Tikhomirov et al. [33] reported that the intrinsic luminescence of Na_2O-ZnO-TeO_2 glasses is associated to bi-coordinated Te and Te—Te bond defects, showing a broad emission with a maximum at 670 nm using a 478 nm excitation light. Thus, defects associated to TeO_2 in the glasses under study are also to be considered. Another aspect of the emission in these glasses can be related to the change in CdO role from a modifier to a glass former. In the literature, cadmium oxide in its crystalline form presents oxygen vacancies and interstitial Cd^{2+}, and these defects increase when the oxide is doped with other metallic ions [24]. On the other hand, Cd ions modify the field strength of Te and Ge due to its polarizability effect and the Cd d^{10} configuration [24]. Therefore, further photoluminescence emission and excitation characterization together with decay times are needed to understand the origin of CdO-TeO_2-GeO_2 glass emission.

To explore possible applications of the fabricated glasses, chromatic coordinates (**Table 4**) were calculated and are depicted in the CIE 1931 chromaticity diagram in **Figure 9**. Global emission of the glasses covers a wide range of colors from sample C10 to C70 that are in the yellow and orange region and C80 that has a white light emission with chromatic coordinates of x = 0.3299 and y = 0.3158, closer to the ideal x = 0.33 and y = 0.33. According to these results, CdO-TeO_2-GeO_2 glasses could be doped with rare earth ions and be potentially used as phosphors for solid state lighting devices.

3.8. $Cd_3Al_2Ge_3O_{12}$ garnet characterization

It is worth to mention that garnets are complex crystal structures with an $A_3B_2(XO_4)_3$ formula, where A is a divalent cation with dodecahedral coordination, B is a trivalent cation of octahedral coordination, and X is a tetravalent cation (Si^{4+}, Ge^{4+}) in tetrahedral coordination.

Sample	x	y
C10	0.3444	0.3961
C20	0.3678	0.4235
C30	0.3755	0.4221
C40	0.3373	0.3851
C50	0.4440	0.4979
C60	0.4993	0.4953
C70	0.3414	0.4089
C80	0.3299	0.3158

Table 4. Estimated chromatic coordinates of the glasses as a function of CdO content.

http://dx.doi.org/10.5772/intechopen.73295

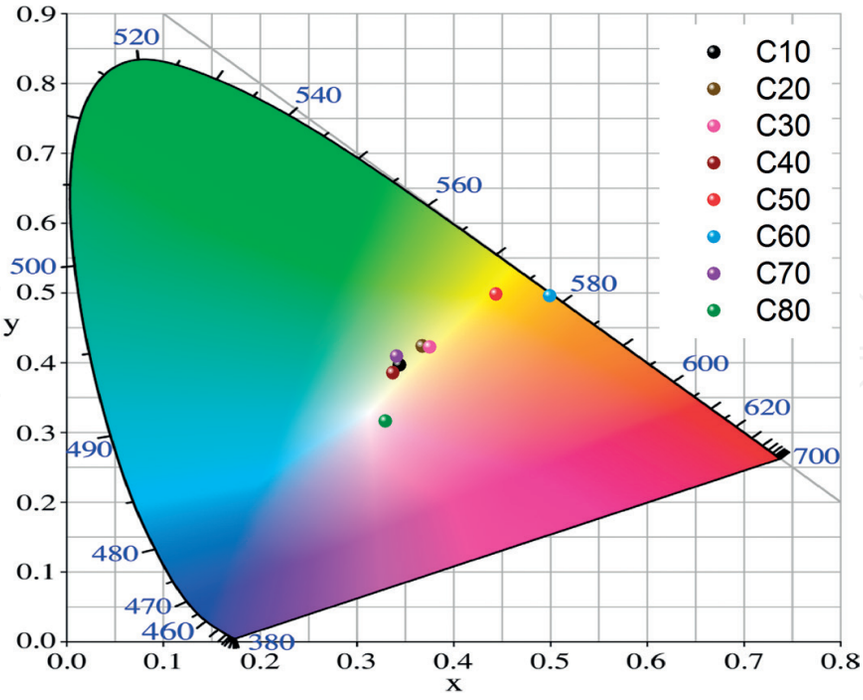

Figure 9. Chromatic coordinates of the glass emission on the CIE 1931 chromaticity diagram where the emission color of the glasses varies along the white, yellow, and yellowish-orange region.

Silicate garnets are found in nature and have a variety of colors depending on the divalent and trivalent cations that constitute the crystal. There are also nonsilicate garnets like the yttrium aluminum garnet (YAG), $Y_3Al_5O_{12}$, and Ce^{3+} doped YAG has a red emission under blue light excitation and is used for lasers [34]. Thus, garnet crystals have potential to be used as phosphors because of their photoluminescence properties as it was previously reported for Ce^{3+} and Mn^{2+} doped silicate and germanate glasses [25]. In a previous Section 3.2.1 in **Figure 3**, the diffraction pattern of C70 glass exhibited the crystalline nature of the sample, and we confirmed the formation of a $Cd_3Al_2Ge_3O_{12}$ garnet. In this section, transmission electron microscopy (TEM) and PL characterization of this crystalline sample are presented.

3.9. TEM

TEM micrographs at different magnifications where phase separation with a droplet distribution in the glass matrix are displayed in **Figure 10a** and **b**. Those droplets are nanocrystals, and at higher magnification, a periodic arrangement is visible in **Figure 10c**. The measured interplanar distance is 2.75 Å that corresponds to the (420) plane in $Cd_3Al_2Ge_3O_{12}$. As a comparison, the Laue diffraction pattern of the nanocrystals overlapped with XRD diffraction pattern is presented in **Figure 10d**, showing the matching of the most intense diffraction peaks related to (420), (422), and (444) Miller indexes of the $Cd_3Al_2Ge_3O_{12}$ garnet. Thus, sample C70 is a nanostructured material composed by the garnet nanocrystals embedded in a glassy matrix.

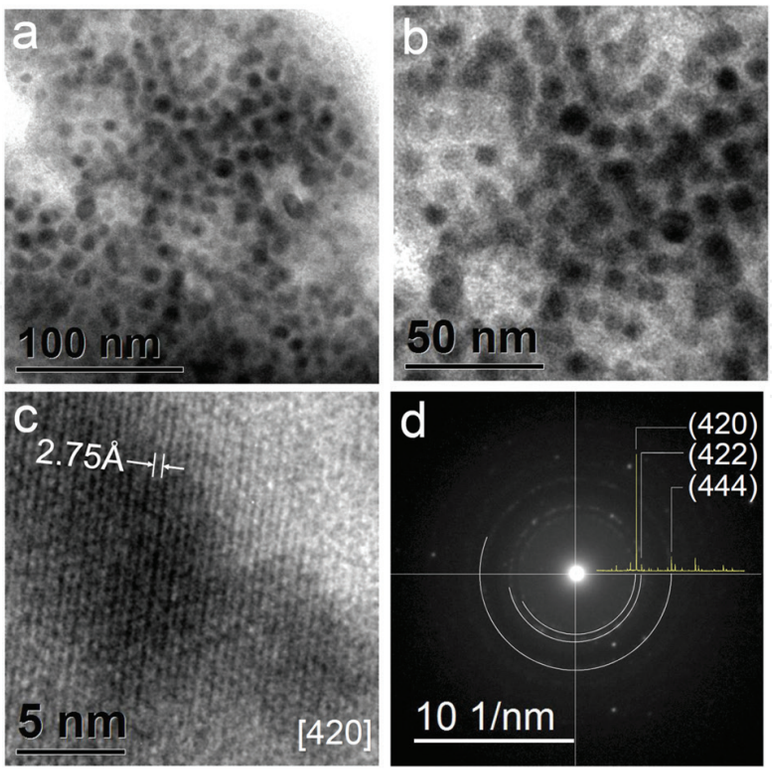

Figure 10. (a and b) Micrographs of sample C80 showing phase separation with a droplet distribution of the nanocrystals, (c) HR-TEM micrograph of the nanocrystals and measuring of the interplanar distance, (d) Laue diffraction pattern comparison with XRD diffraction pattern of sample C70.

3.10. Photoluminescence

Lui et al. [35] have previously reported the synthesis of $Cd_3A_{l2}Ge_3O_{12}$ doped with Dy^{3+} ions and its afterglow properties. In their work, emission of the doped garnet under a 254 nm excitation light shows a broad band overlapped with the $^4F_{9/2} \rightarrow {}^6H_{15/2}$ and $^4F_{9/2} \rightarrow {}^6H_{13/2}$ emission transitions of Dy^{3+} at 485 and 580 nm, respectively. Then, as comparison, our sample was excited with the same wavelength, the same wavelength to excite our crystallized sample was used, and the resulting spectrum is displayed in **Figure 11a**. The spectrum consists of a very broad band in the visible spectral range (400–750 nm) with a maximum at 526 nm. In the previous report, the emission band maximum of the Dy doped garnet is located at ~430 nm. The authors proposed two possible origins of the intrinsic garnet emission: the formation of Cd^{2+} vacancies during processing and the presence of $(GeO_4)^{4+}$ tetrahedral groups [35, 36]. However, $(GeO_4)^{4+}$ group emission is around 310 nm as it was reported for the $Ca4ZrGe_3O_{12}$ garnet [37]. Moreover, the GeO_2 emission is in the UV range and it was discussed previously. It is reported that germanate compounds like $SrGeO_3:Eu^{3+}$, $NaLa_9(GeO_4)_6O_2$, and rare earth doped garnets like $\{Ca(Tb)\}_3Ga_2Ge_3O_{12}$ and $Sr_3[Y(Tb)]_2Ge_3O_{12}$ are of interest to be employed as red-light phosphors for near-ultraviolet-white light emitting diodes and field-emission displays (NUV-WLEDs and FEDs) [38–40]. Chromaticity coordinates of the intrinsic luminescence of cadmium aluminum germanate were estimated (x = 0.3267, y = 0.4795) and are presented in the CIE 1931 color space in **Figure 11b**, as it can be seen that the emission color is in the yellowish-green region.

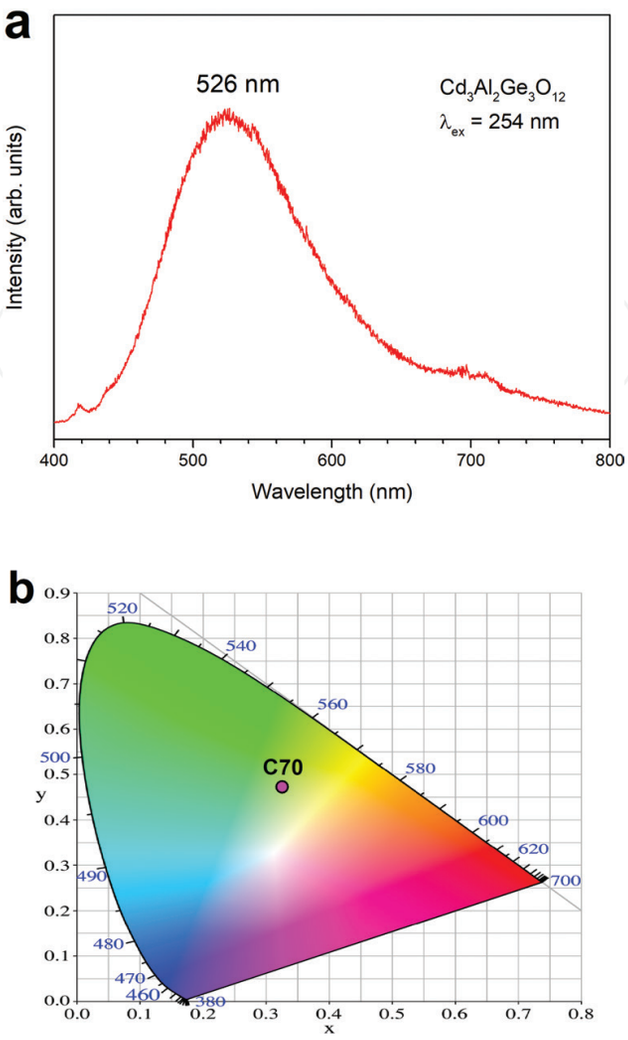

Figure 11. (a) Emission spectra of the C70 crystallized sample monitored using a 254 nm laser. (b) Chromatic coordinates of C70 light emission on the CIELAB 1931 color space, which are in the yellowish-green region.

4. Summary

A series of yellowish transparent glasses of the CdO-TeO_2-GeO_2 system were obtained even at high CdO content. Thus, CdO changes its role from modifier to network former. Incorporation of aluminum through crucible corrosion leads to the formation of the $Cd_3A_{l2}Ge_3O_{12}$ garnet at 60 and 70 wt% of CdO. The glasses were structurally characterized by XRD, Raman, and XPS spectroscopies demonstrating that their structure is complex and undergoes several changes as the CdO content increases, and this behavior affects the energy band gap values. Luminescence of the glasses demonstrates several structural changes that the samples undergo with concentration variation, showing a very broad structured emission band in the range of visible light monitored with a 370 nm excitation wavelength. The defects that cause the emission of the glasses are yet to be understood and studied. Chromatic coordinates show that emission color of the glasses varies in the range of yellow to orange. The glass with CdO 80 wt% global emission lies in the white light region of the CIE 1931 chromaticity diagram with x = 0.3299 and

y = 0.3158 values. Thus, these series of glasses are good candidates for optoelectronic devices or as rare earth ion hosts. The $Cd_3Al_2Ge_3O_{12}$ garnet is nanostructured as it was determined by TEM analysis, and PL measurements shows a broad emission centered at 526 nm with calculated chromatic coordinates of x = 0.3267, y = 0.4795, which lies in the yellowish-green region of the CIE 1931 chromatic diagram. Previous reports in the literature show that garnet structures doped with rare earth ions, especially germanates, are of interest for their applications as phosphors in optoelectronic devices. Further research is needed to fully understand the structure and hence the optical properties of glasses of the $CdO\text{-}TeO_2\text{-}GeO_2$ system.

Acknowledgements

The authors thank CONACYT for their financial and fellowship support of Cátedra-CONACYT (1959) project.

Author details

Josefina Alvarado Rivera[1]*, Carlos Guadalupe Pérez Hernández[2], María Elena Zayas[3] and Enrique Álvarez[2]

*Address all correspondence to: josefina.alrive@gmail.com

1 CONACYT-University of Sonora, Hermosillo, Sonora, Mexico

2 Physics Department, University of Sonora, Hermosillo, Sonora, Mexico

3 Physics Research Department, University of Sonora, Hermosillo, Sonora, Mexico

References

[1] Rachkovskaya GE, Zakharevich GB. IR spectra of tellurium germanate glasses and their structure. Journal of Applied Spectroscopy. 2007;**74**(1):86-89. DOI: 10.1007/s10812-007-0013-z

[2] El-Mallawany RAH. Handbook of Tellurite Glasses—Physical Properties and Data. CRC Press: USA; 2011

[3] Goldschmidt VM. Skriffer Norke Videnskaps Akad. Oslo I, Mathematisch-Naturwiss. Klasse. 1926;**1**:7

[4] Carter CB, Norton MG. Ceramic Materials Science and Engineering. New York: Springer; 2007

[5] Tcheivili L. Un vidrio de fluoruro de plomo (A lead fluoride glass). Boletín de la Sociedad Española de Cerámica. 1968;Agosto-Julio:461-473

[6] Stevels JM. The glass considered as a polymer. Glass Industry. 1954;**35**(2):69-72

[7] Walter G, Vogel J, Hoppe U, Hartmann P. The structure of $CaO-Na_2O-MgO-P_2O_5$ invert glass. Journal of Non-Crystalline Solids. 2001;**296**(3):212-223. DOI: 10.1016/S0022-3093(01)00912-7

[8] Feng X, Tanabe S, Hanada T. Spectroscopic properties and thermal stability of Er^{3+} doped germanotellurite glasses for broadband fiber amplifiers. Journal of the American Ceramic Society. 2001;**84**(1):165-171. DOI: 10.1111/j.1151-2916.2001.tb00625.x

[9] Henderson S. The germanate anomaly: What do we know? Journal of the Non-Crystalline Solids. 2007;**353**(18-21):1695-1704. DOI: 10.1016/j.jnoncrysol.2007.02.037

[10] Alvarado-Rivera J, Rodríguez-Carvajal DA, Acosta-Enríquez MC, Manzanares-Martínez MB, Álvarez E, Lozada-Morales R, Díaz GC, et al. Effect of CeO_2 on the glass structure of sodium germanate glasses. Journal of the American Ceramic Society. 2014;**97**(11):3493-3500. DOI: 10.1111/jace.13202

[11] Sreenivasulu V, Upender G, Mouli VC, Prasad M. Structural, thermal and optical properties of TeO_2-ZnO-CdO-BaO glasses doped with VO^{2+}. Spectrochimica Acta Part A: Molecular and Biomolecular Spectroscopy. 2015;**148**:215-222. DOI: 10.1016/j.saa.2015.03.085

[12] Grado-Caffaro MA, Grado-Caffaro M. A quantitative discussion on band-gap energy and carrier density of CdO in terms of temperature and oxygen partial pressure. Physics Letters A. 2008;**372**(27-28):4858-4860. DOI: 10.1016/j.physleta.2008.04.068

[13] Brady GW. Structure of tellurium oxide glass. Journal of Chemical Physics. 1957;**27**:300. DOI: 10.1063/1.1743690

[14] Upender G, Vardhani CP, Suresh S, Awasthi AM, Mouli VC. Structure, physical and thermal properties of WO_3-GeO_2-TeO_2 glasses. Materials Chemistry and Physics. 2010;**125**(1-2):335-341. DOI: 10.1016/j.matchemphys.2010.01.050

[15] Ersundu AE, Çelikbilek M, Solak N, Aydin S. Glass formation area and characterization studies in the $CdO-WO_3-TeO_2$ ternary system. Journal of the European Glass Ceramic Society. 2011;**31**(15):2775-2781. DOI: 10.1016/j.jeurceramsoc.2011.07.027

[16] Yang Z, Xu S, Yang J, Hu L, Jiang Z. Thermal analysis and optical transition of Yb^{3+}, Er^{3+} co-doped lead-germanium-tellurite glasses. Journal of Materials Research. 2004;**19**(6):1630-1637. DOI: 10.1557/JMR.2004.0226

[17] Ma L, Chen Y, Wei Z, Cai H, Zhang F, Wu X. Facile method to prepare CdS nanostructure bases on the CdTe films. Applied Surface Science. 2015;**349**(15):740-745. DOI: 10.1016/j.apsusc.2015.05.024

[18] Dzhagan V, Lokteva I, Himcinschi C, Jin X, Kolny-Olesiak J, Zahn DR. Phonon Raman spectra of colloidal CdTe nanocrystals: Effects size, non-stoichiometry and ligand exchange. Nanoscale Research Letters. 2011;**6**(1). DOI: 10.1186/1556-276X-6-79

[19] Rachokoskaya GE, Zakharevich GB. Germanate lead-tellurite glasses for optical light filters. Glass and Ceramics. 2012;**68**(11-12):385-388. DOI: 10.1007/s10717-012-9396-2

[20] Culea E, Pop L, Bosca M, Rusu T, Pascuta P, Rada S. FTIR spectroscopic study of some lead germanate glasses. Journal of Physics: Conference Series. 2009;**182**(1):012061

[21] Monteiro G, Santos LF, Pereira JCG, Almeida RM. Optical and spectroscopic properties of germanotellurite glasses. Journal of Non-Crystalline Solids. 2011;**357**(14):2695-2701. DOI: 10.1016/j.jnoncrysol.2010.12.062

[22] Tripathi R, Dutta A, Das S, Kumar A, Sinha TP. Dielectric relaxation of CdO nanoparticles. Applied Nanoscience. 2016;**6**(2):175-181. DOI: 10.1007/s13204-015-0427-5

[23] Lucacel RC, Marcus C, Ardelean I. FTIR and Raman spectroscopic studies of copper doped $2GeO_2$.PbO.Ag_2O glasses. Journal of Optoelectronics and Advanced Materials. 2007;**9**(3):747-750

[24] Moholkar AV, Agawane GL, Sim KU, Kwon YB, Choi DS, Rajpure KY, Kim JH. Temperature dependent structural, luminescent and XPS studies of CdO:Ga thin films deposited by spray pyrolysis. Journal of Alloys and Compounds. 2010;**506**(2):794-799. DOI: 10.1016/j.jallcom.2010.07.072

[25] Salim MA, Khattak GD, Tabet N, Wenger LE. X-ray photoelectron spectroscopy (XPS) studies of copper-sodium tellurite glasses. Journal of Electron Spectroscopy and Related Phenomena. 2003;**128**(1):75-83. DOI: 10.1016/S0368-2048(02)00214-1

[26] Lim JW, Jain H, Toulouse J, Marjanovic S, Sanghera JS, Miklos R, Aggarwal ID. Structure of alkali tungsten tellurite glasses by X-ray photoelectron spectroscopy. Journal of Non-Crystalline Solids. 2004;**349**:60-45. DOI: 10.1016/j.jnoncrysol.2004.08.263

[27] Castro-Rodríguez R, Iribarren A, Bartolo-Pérez P, Peña JL. Obtaining of polycrystalline $CdTeO_3$ by reactive pulse laser deposition. Thin Solid Films. 2005;**484**(1):100-103. DOI: 10.1016/j.tsf.2005.02.011

[28] Mekki A, Holland D, Ziq KA, McConville CF. Structural and magnetic properties of sodium iron germanate glasses. Journal of Non-Crystalline Solids. 2000;**272**(2):179-190. DOI: 10.1016/S0022-3093(00)00235-0

[29] Moulder FJ. X-Ray Photoelectron Spectroscopy: A Reference Book of Standard Spectra for Identification and Interpretation of XPS Data. Eden Prairie, Minnesota: Physical Electronics Division, Perkin-Elmer Corporation; 1992

[30] Gowrishankar S, Balakrishnan L, Gopalakrishnan N. Band gap engineering in Zn(1−x)CdxO and Zn(1−x)MgxO thin films by RF sputtering. Ceramics International. 2014;**40**(1):2135-2142. DOI: 10.1016/j.ceramint.2013.07.130

[31] Duman S, Turgut G, Özçelik FŞ, Gurbulak B. The synthesis and characterization of sol-gel spin coated CdO thin films: As a function of solution molarity. Materials Letters. 2014;**126**:232-235. DOI: 10.1016/j.matlet.2014.04.063

[32] Wada N, Mayu I, Kojima K. Glass composition dependence of luminescence due to Ge^{2+} center in germanate glasses. Journal of Non-Crystalline Solids. 2006;**352**(23):2657-2661. DOI: 10.1016/j.jnoncrysol.2006.02.073

[33] Tikhomirov VK, Ronchin S, Montagna M, Ferrari M, Furniss D. Intrinsic defect related photoluminescence in TeO_2-based glasses. Physica Status Solidi A. 2001;**187**(11):R4-R6. DOI: 10.1002/1521-396X(200109)187:1<R4::AID-PSSA99994>3.0.CO;2-6

[34] He X, Liu X, Li R, Yang B, Yu K, Zeng M, Yu R. Effects of local structure of Ce^{3+} ions on luminescent properties of $Y_3Al_9O_{12}$:Ce nanoparticles. Scientific Reports. 2016;**6**:22238. DOI: 10.1038/srep22238

[35] Lui Z, Liu Y. Afterglow energy transfer in $Cd_3Al_2Ge_3O_{12}$:Dy. Physica Status Solidi A. 2005;**202**(9):1814-1817. DOI: 10.1002/pssa.200420034

[36] Blasse G, Bril A. Fluorescence of Eu^{3+} activated-garnets containing pentavalent vanadium. Journal of Electrochemistry. 1967;**114**(3):250-252. DOI: 10.1149/1.2426560

[37] Blasse G, De Blank J, IJdo DJW. The luminescence of the garnet $Ca_4ZrGe_3O_{12}$. Materials Research Bulletin. 1995;**30**(7):845-850. DOI: 10.1016/0025-5408(95)00068-2

[38] Wang T, Xu X, Zhou D, Qiu J, Yu X. Luminescent properties of $SrGeO_3$:Eu^{3+} red emitting phosphors for field emission displays. ECS Journal of Solid State Science and Technology. 2014;**3**(8):R139-R143. DOI: 10.1149/2.0081408jss

[39] Cao Y, Zhu G, Wang Y. Synthesis, structure and luminescence characteristics of a novel red phosphor $NaLa_9(GeO_4)_6O_2$:Eu^{3+} for light emitting diodes and field emission displays. RSC Advances. 2015;**5**(81):65710-65718. DOI: 10.1039/C5RA10435A

[40] Avouris P, Chang IF, Duvgneaud PH, Giess EA, Morgan TN. Luminescence of germanate garnets with terbium on dodecahedral and octahedral lattices sites. Journal of Luminescence. 1982;**26**(3):213-225. DOI: 10.1016/0022-2313(82)90049-7

IntechOpen